The Astrophysical Journal, 812:166 (7pp), 2015 October 20 doi:10.1088/0004-637X/812/2/166

ULTRA-LUMINOUS X-RAY SOURCES IN HARO 11 AND THE ROLE OF X-RAY BINARIES IN FEEDBACK IN Lyα EMITTING GALAXIES

A. H. Prestwich[1], F. Jackson[2], P. Kaaret[3], M. Brorby[3], T. P. Roberts[4], S. H. Saar[1], and M. Yukita[5]
[1] Harvard-Smithsonian Center for Astrophysics, 60 Garden Street, Cambridge, MA 02138, USA
[2] Department of Physics and Astronomy, University of Toledo, 2801 West Bancroft Street, Toledo, OH 43606, USA
[3] Department of Physics and Astronomy, University of Iowa, Van Allen Hall, Iowa City, IA 52242, USA
[4] Department of Physics, University of Durham, South Road, Durham DH1 3LE, UK, USA
[5] Johns Hopkins University, Homewood Campus, Baltimore, MD 21218, USA
Received 2013 October 1; accepted 2015 July 23; published 2015 October 20

ABSTRACT

Lyman Break Analogs (LBAs) are local proxies of high-redshift Lyman Break Galaxies. Spatially resolved studies of nearby starbursts have shown that Lyman continuum and line emission are absorbed by dust and that the Lyα is resonantly scattered by neutral hydrogen. In order to observe Lyα emission from star-forming regions, some source of feedback is required to blow the neutral gas away from the starburst to prevent scattering and allow the Lyα emission to escape. We show that there are two X-ray point sources embedded in the diffuse emission of the LBA galaxy Haro 11. CXOU J003652.4-333316 (abbreviated to Haro 11 X-1) is an extremely luminous ($L_X \sim 10^{41}$ erg s^{-1}), spatially compact source with a hard-X-ray spectrum. We suggest that the X-ray emission from Haro 11 X-1 is dominated by a single accretion source. This might be an active galactic nucleus or a source similar to the extreme black hole binary (BHB) M82 X-1. The hard X-ray spectrum indicates that Haro 11 X-1 may be a BHB in a low accretion state. In this case, the very high X-ray luminosity suggests an intermediate mass black hole that could be the seed for formation of a supermassive black hole. Source CXOU J003652.7-33331619.5 (abbreviated Haro 11 X-2) has an X-ray luminosity of $L_X \sim 5 \times 10^{40}$ erg s^{-1} and a soft X-ray spectrum (power-law photon index $\Gamma \sim 2.2$). This strongly suggests that Haro 11 X-2 is an X-ray binary in the ultra luminous state (i.e., an Ultra Luminous X-ray source, ULX). Haro 11 X-2 is coincident with the star-forming knot that is the source of the Lyα emission. The association of a ULX with Lyα emission raises the possibility that strong winds from X-ray binaries play an important role in injecting mechanical power into the interstellar medium, thus blowing away neutral material from the starburst region and allowing the Lyα to escape. We suggest that feedback from X-ray binaries may play a significant role in allowing Lyα emission to escape from galaxies in the early universe.

Key words: galaxies: clusters: general – galaxies: dwarf – galaxies: starburst – X-rays: binaries – X-rays: galaxies

1. INTRODUCTION

The youngest galaxies in the early universe are strong sources of Lyα and Lyman continuum emission from young, massive stars (Steidel et al. 1999, and references therein, Shapley et al. 2006; Nilsson et al. 2007; Mallery et al. 2012). These are the systems thought to be responsible for reionizing the early universe (Haiman & Spaans 1999; Dijkstra et al. 2007; Mesinger & Furlanetto 2008; Fontanot et al. 2012). Two techniques are used to discover large numbers of galaxies at high redshifts: the direct detection of Lyα emission in a narrow band filter (Hu & McMahon 1996; Gronwall et al. 2007; Ouchi et al. 2008; Mallery et al. 2012) and the Lyman Break technique (Steidel et al. 1995, 1996, 1999). The Lyman Break technique makes use of the fact that star-forming galaxies have spectral energy distributions that exhibit a large drop in flux at wavelengths shorter than the Lyman limit in the rest frame of the galaxy (Steidel et al. 1995). The Lyman break is likely due to a combination of the intrinsic spectral shape of the young stellar population and absorption by neutral gas. Deep imaging of objects above and below the Lyman limit can identify objects that disappear at shorter wavelengths: this "dropout" is likely due to the Lyman break (Steidel et al. 1995). Objects discovered via their Lyα emission are referred to as Lyα Emitters (LAEs), and those identified via the Lyman break as Lyman Break Galaxies (LBG).

Despite the importance of Lyman emission, both for high-redshift surveys and for understanding galaxy evolution, the details of how Lyman emission escapes from a galaxy are not well understood. This is because Lyα line and continuum emission cannot be spatially resolved in high-redshift systems. To address this problem, Heckman et al. (2005) and Hoopes et al. (2007) derived a sample of compact, UV bright, low-redshift galaxies using *GALEX* and the Sloan Digital Sky Survey. These galaxies have properties that are very similar to LBG, including size, UV luminosity, surface brightness, mass, star-formation rate, and metallicity (Heckman et al. 2005; Hoopes et al. 2007). They are known as Lyman Break Analogs (LBA) and are used as proxies of high-redshift LBG. Spatially resolved studies of local starburst galaxies have shown that Lyman continuum and line emission is absorbed by dust, reducing the Lyα line strength from values predicted by simple models of H II regions (Kunth et al. 2003; Mas-Hesse et al. 2003; Östlin et al. 2009; Scarlata et al. 2009). In addition, the Lyα is resonantly scattered by neutral hydrogen surrounding the starburst region (Neufeld 1991; Hayes et al. 2010; Verhamme et al. 2012 and references therein). It appears that some source of feedback is required to blow the neutral gas away from the starburst to prevent scattering and allow the Lyα emission to escape (Orsi et al. 2012; Wofford et al. 2013). The most obvious source of mechanical power is supernovae and stellar winds from the starburst region creating "super-bubbles" (Tenorio-Tagle et al. 1999; Hayes et al. 2007; Heckman et al. 2011).

Haro 11 is a famous compact dwarf galaxy undergoing an intense starburst that has been intensively studied at all

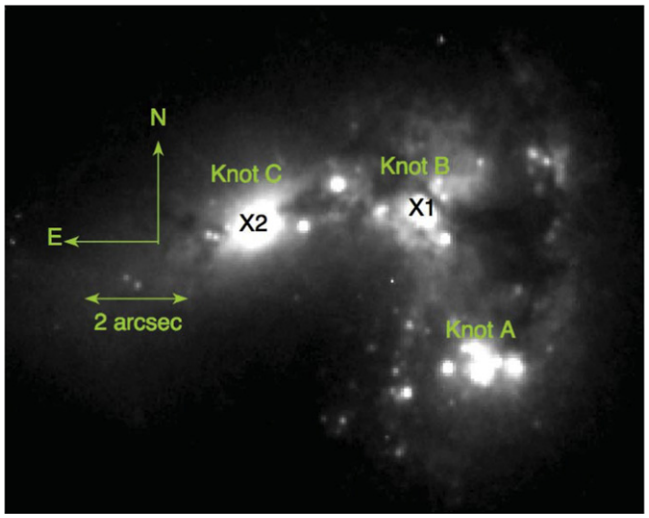

Figure 1. Image of Haro 11 showing the three star-forming knots identified by Vader et al. (1993). Also shown are the locations of the two bright X-ray point sources Haro 11 X-1 and Haro 11 X-2. The image was taken by the *Hubble Space Telescope* (*HST*) Advanced Camera for Surveys Wide Field Camera in F435W ban and downloaded from the Hubble Legacy Archive.

wavelengths (see Adamo et al. 2010, and references therein). The starburst region is resolved into three distinct knots, labeled A, B, and C by Vader et al. (1993; see Figure 1). It is an LAE emitter (Kunth et al. 2003) and is in the Hoopes et al. (2007) sample of LBA. In addition, Haro 11 is the only known example of a local Lyman continuum emitter (Leitet et al. 2011). The Lyα emission is centered on a massive star-forming region (Knot C). Grimes et al. (2007) studied the global X-ray emission of Haro 11. They showed that the X-ray emission is spatially extended and that the integrated spectrum of the entire galaxy is composed of a diffuse thermal component associated with hot gas and a power-law component likely associated with the X-ray binary population of the galaxy (Grimes et al. 2007).

In this paper, we study the X-ray properties of two point sources in Haro 11. CXOU J003652.4-333316 (abbreviated to Haro 11 X-1) is an extremely luminous ($L_X \sim \times\ 10^{41}$ erg s^{-1}) source with a hard-X-ray spectrum that is coincident with Knot B. We suggest that the X-ray emission from Haro 11 X-1 is dominated by a single accretion source. This might be an active galactic nucleus (AGN) or a source similar to the extreme black hole binary (BHB) M82 X-1. The hard-X-ray spectrum indicates that Haro 11 X-1 may be a BHB in a low accretion state (McClintock & Remillard 2006; Remillard & McClintock 2006). If this is the case, the very high X-ray luminosity suggests an intermediate mass black hole (IMBH). If this interpretation is correct, Haro 11 X-1 is an extremely unusual object. Finally, we note that an IMBH in a young galaxy may form the seed for a supermassive black hole—we may be witnessing the birth of an AGN in Haro 11.

Source CXOU J003652.7-33331619.5 (Haro 11 X-2) is coincident with Knot C, also at the center of the Lyα emission. The X-ray luminosity of Haro 11 X-2 and the soft-X-ray spectrum suggests that it is an Ultra Luminous X-ray (ULX). ULXs are known to have powerful jets and winds that impact their environment (Pakull & Mirioni 2002; Abolmasov et al. 2007; Abolmasov 2011). The fact that a ULX is coincident with Knot C raises the possibility that winds from the compact object may play a significant role in sweeping up

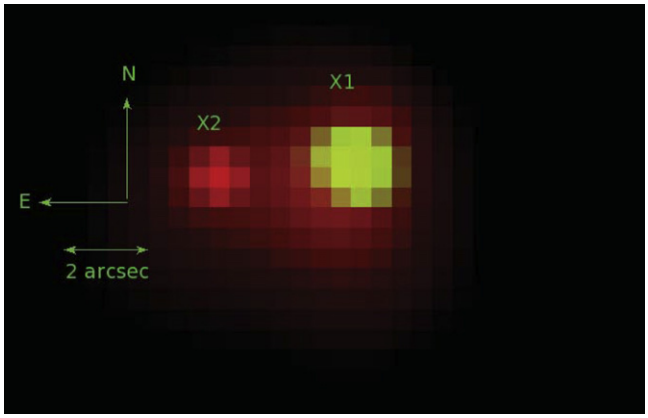

Figure 2. Two band (0.3–1 keV = red and 3–5 keV = green) false color image of the X-ray emission. The two point sources, Haro 11 X-1 and Haro 11 X-2, are shown.

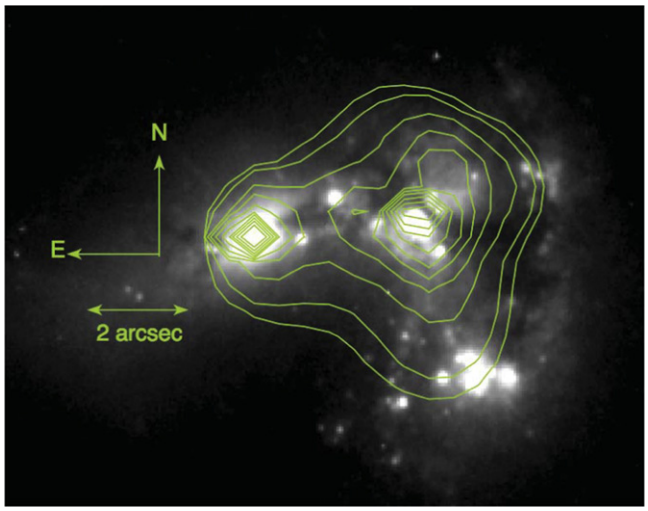

Figure 3. X-ray contours (0.3–5 keV) superimposed on the *HST* optical image.

the neutral gas and allowing the Lyα to escape. We suggest that feedback from X-ray binaries may be significant in the early universe (Justham & Schawinski 2012; Fragos et al. 2013; Pacucci et al. 2014).

We adopt a distance of $D = 84.0$ Mpc to Haro 11 resulting in a scale of 407 pc arcsec^{-1} (NASA Extrgalactic Database).

2. X-RAY OBSERVATIONS

Haro 11 was observed with the *Chandra* ACIS-S array for 54 ks on 2006 October 28, obsid 8175. Data were reprocessed using CIAO version 4.5 and CALDB 4.5.5.1.

A two-band (0.3–1 keV = red and 3–5 keV = green) false color X-ray image of Haro 11 is shown in Figure 2. Two bright point sources are visible, one of which (Haro 11 X-1) has a hard spectrum and is clearly visible in the 3–5 keV band. There is a second point source visible (Haro 11 X-2) to the east of Haro 11 X-1. There is also extended soft-X-ray emission. Figure 3 shows the location of the X-ray emission (red contours) relative to star-forming Knots A, B, and C discussed by Vader et al. (1993), Kunth et al. (2003), and Adamo et al. (2010). The source Haro 11 X-1 is associated with Knot B and Haro 11 X-2 is associated with Knot C. Figure 4 shows the Lyα emission from Östlin et al. (2009) with X-ray contours

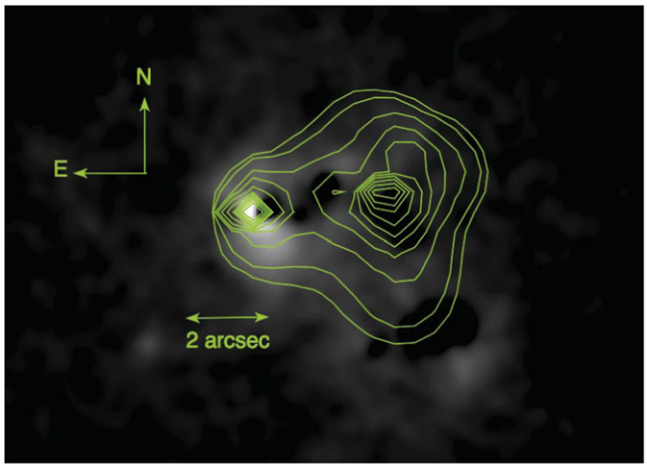

Figure 4. X-ray contours (0.3–5 keV) superimposed on the Lyα line emission (Östlin et al. 2009). The Lyα image is continuum subtracted. The ULX Haro 11 X-2 is associated with Knot C and the Lyα line emission. Haro 11 X-1 is associated with Knot B.

superimposed. The bulk of the Lyα line emission is associated with Knot C and Haro 11 X-2.

2.1. Spectral Analysis of the Point Sources

Spectra were extracted for both of the point sources (Haro 11 X-1 and Haro 11 X-2) in the range of 0.3–10 keV, using the *CIAO* tool *dmextract*. Spectra were also extracted from annular background regions (inner radius $= r_1$, outer radius $= r_2$) centered on the sources. The source and background extraction radii were chosen by visual inspection of the sources. Details of the extraction regions used are in Table 1. *Sherpa* was used to fit the spectra in the 0.5–8 keV range. The spectra were grouped with a minimum of 15 counts per bin and fit with an absorbed power law (*Sherpa* syntax xswabs*powlaw1d). For both fits, the absorption was allowed to vary, but not to drop below the galactic value of 1.88×10^{-20} cm^{-2} (Dickey & Lockman 1990). The best-fit spectra are shown in Figure 5. Both sources are well fit with an absorbed power law. The best-fit spectrum of Haro 11 X-1 is hard, with a power-law slope of $\Gamma = 1.2 \pm 0.2$ (Table 1).

3. THE NATURE OF HARO 11 X-1

Haro 11 X-1 is an unusual source. Most of the emission appears to come from a spectrally hard unresolved source with X-ray luminosity $L_X \sim 10^{41}$ erg s^{-1}. This is very high for a single X-ray binary, and is comparable to the IMBH candidate HLX-1 (Servillat et al. 2011). This source is coincident with star-forming Knot B.

3.1. The Spatial Extent of Haro 11 X-1

The X-ray luminosity of Haro 11 X-1 is very high for a single X-ray binary and has a hard spectrum. We therefore consider whether it is powered by an AGN, one or more X-ray binary or other high energy processes associated with star formation (e.g., such as outflowing gas from a starburst region (Yukita et al. 2012), inverse Compton scattering of infrared photons off of relativistic electrons (Hargrave 1974; Rieke et al. 1980), or synchrotron from very high energy electrons (Lacki & Thompson 2013)). In this section, we put observational constraints on the X-ray spatial extent of Haro 11 X-1. If

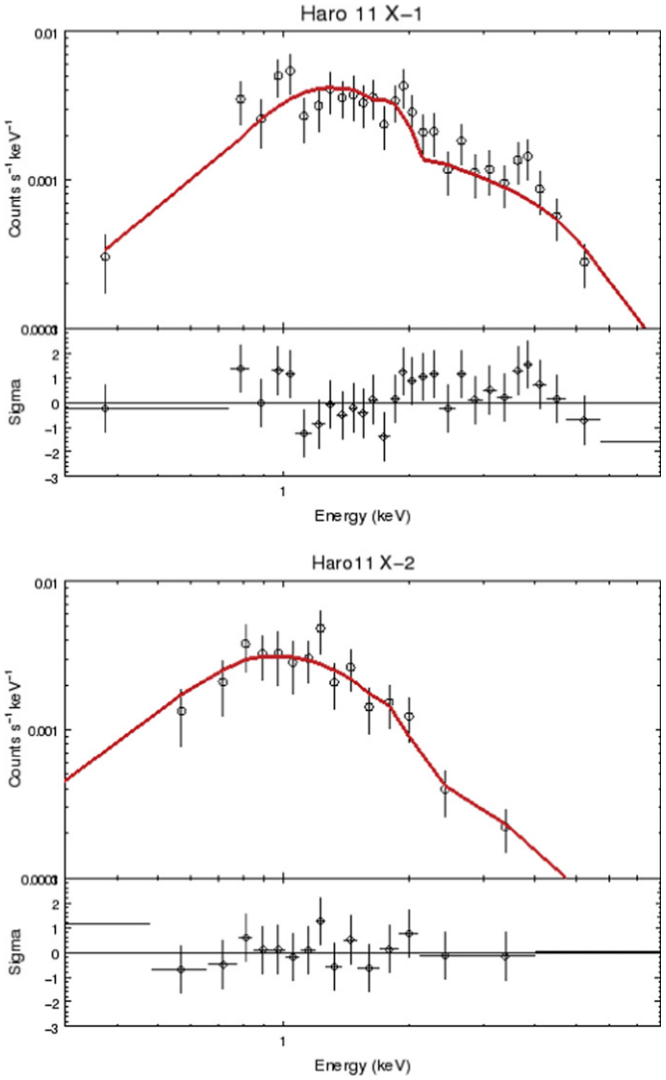

Figure 5. Best-fit X-ray spectra and residuals for the two bright point sources. The top panel shows Haro 11 X-1 and the bottom panel shows Haro 11 X-2. The best-fit models are shown in red. Best-fit models are shown in Table 1.

the source is extended, we can definitively say that not all of the X-ray flux comes from a single accretion source. We note that at the distance of Haro 11, one arcsecond corresponds to approximately 400 pc. Failure to detect spatial extent does not rule out a contribution from an extended component.

We compare the radial profile of Haro 11 X-1 in the 3–5 keV band with a monochromatic point response function (PSF) at 4 keV (generated using ChaRT). The 3–5 keV band was chosen because the thermal hot gas (kT$\sim$1 keV) contributes very little flux above 3 keV and the flux from Haro 11 X-1 drops off rapidly above 5 keV. The source and PSF images were binned at 0.25 arcsec pixel^{-1}. We used *Sherpa* two-dimensional fitting routines to obtain the best-fit PSF. The PSF generated from ChaRT was used as the convolution kernel and a 2D Delta function (i.e., a point source) used as the model. The best-fit scaled PSF was obtained. We then obtained the radial profile of the PSF and fit it with a 1D Gaussian to derive a 1D PSF. Parameters of the 1D PSF are shown in Table 2. The radial profile of Haro 11 was fit with a model comprising the 1D PSF plus a constant background. The background was calculated to be 0.2 counts arcsec^{-2}. This is a combination of instrument

Table 1
Extraction Regions and Best-fit Spectral Parameters

	Haro 11 X-1	Haro 11 X-2
R.A.	00:36:52.42	00:36:52.70
Decl.	−33:33:16.95	−33:33:16.95
Extraction radius (arcsec)	1.1	1.1
Background annulus, r_1–r_2(arcsec)	3.6–4.8	1.2–2.3
Source Counts	472	232
Background Counts	291	60
Model	PL	PL
N_H ($\times 10^{20}$ cm^{-2})	$18.8^{+14.6}_{-12.7}$	$14.8^{+9.9}_{9.9}$
Γ	$1.2^{+0.2}_{-0.2}$	$2.2^{0.4}_{-0.4}$
PL Flux[1]	$11.8\ ^{+3.7}_{-4.5}$	$5.5^{+3.7}_{-2.3}$
X-ray Luminosity[2]	$9.9^{+8.4}_{-1.3}$	$4.7^{+6.1}_{-1.0}$
χ^2/dof	19.4/24	5.61/13

[1] $F_X(0.3–8.0\ \mathrm{keV})\times 10^{-14}$ erg s^{-1} cm^{-2}
[2] $L_X(0.3–8.0\ \mathrm{keV})\times 10^{40}$ erg s^{-1}, (not corrected for absorption)

Table 2
Best-fit Spatial Components

Gaussian				
FWHM (arcsec)	Amplitude	Background (cts arcsec^{-2})	χ^2/dof	Note
0.76	41.75	0.2	2.5/9	parameters from PSF, no fit
1.0	41.75	0.51	1.4/7	background and FWHM allowed to change

background (see the *Proposers Observatory Guide V. 16*) plus a contribution from the extended emission from Haro 11. The extended component is composed of thermal emission plus a power-law component. It is the power law that contributes a small amount of flux at 4 keV.

We initially fixed all of the model components (background, Gaussian width, amplitude, and position) with their default values and used *Sherpa* to calculate the χ^2 and χ^2 per degree of freedom (the reduced χ^2). Despite the fact that no parameters were allowed to vary, the PSF plus background was an acceptable fit to the data (reduced $\chi^2 = 0.28$). In order to test the hypothesis that the source may be slightly extended, we allowed the FWHM and background to change during a fit. This improved the fit slightly (Table 2) changing χ^2 from 1.93 to 1.46 (final reduced $\chi^2 = 0.18$. The best-fit Gaussian FWHM is 1.0 arcsec, compared to 0.76 arcsec for the PSF. The radial profile of the compact source, the best-fit and the original keV PSF are shown in Figure 6. We conclude that Haro 11 X-1 is slightly extended beyond the PSF. The extended component contributes ∼4 counts to the 3–5 keV flux (4% of the total 3–5 keV flux).

3.2. Physical Interprtation of Haro 11 X-1

We suggest the X-ray characteristics of Haro 11 X-1 (hard spectrum, compact source, high luminosity) are best explained

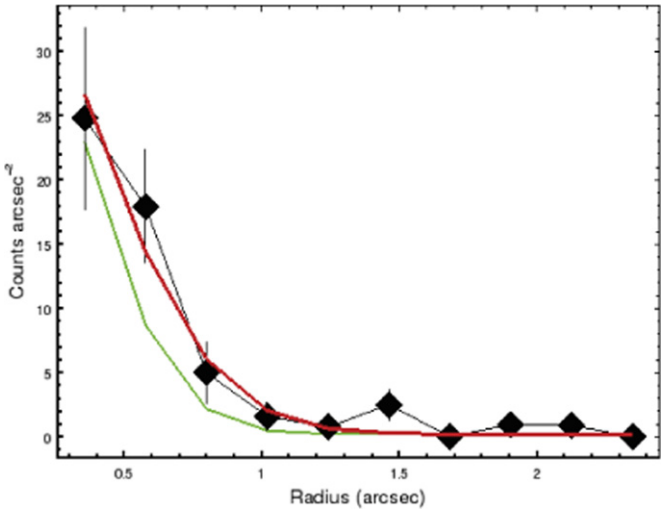

Figure 6. Radial profile of Haro 11 X-1 in the 3–5 keV band (black) compared to the best-fit model. The model was generated by allowing the FWHM of the PSF and the background to vary. A 4 keV point response function generated using ChaRT and scaled to the data is also shown in green. The radial profile of Haro 11 X-1 is slightly broader than the PSF. Parameters of the best-fit spatial model are shown in Table 2.

if the X-ray emission is dominated by a single accretion source. We note that the radial profile fit is improved slightly with a background component in addition to the instrumental background. This background is likely due to high energy processes in starburst regions (e.g., outflowing gas from a starburst region, inverse Compton scattering of infrared photons off of relativistic electrons and synchrotron from very high energy electrons) and unresolved X-ray binaries.

Haro 11 X-1 also appears to be coincident with an unresolved/compact H I absorption feature recently reported by MacHattie et al. (2014). The 21 cm continuum emission peaks at the same location (MacHattie et al. 2014).

3.2.1. Low-luminosity AGN

To our knowledge, there have been no reports of an LLAGN in Haro 11. The optical line ratios are generally consistent with H II regions (Vader et al. 1993; James et al. 2013). The mid-infrared emission lines of low metallicity starbursts are discussed by Hao et al. (2009). They find that the [O IV]25.9 μm/[S III]33 μm and [Ne III]15.56 μm/ [Ne II]12.81 μm ratio is a good discriminator between AGN and starbursts. Haro 11 is well within the starburst region using these diagnostics. Finally, we note that Heisler et al. (1998) observed Haro 11 at 2.3 GHz with the Parkes–Tidbinbilla interferometer, which is sensitive to high surface brightness cores (spatial extent <0.1 arcsec and $T_b > 10^5$ K). No source was detected.

We cannot rule out an LLAGN whose optical and IR signature is diluted by the intense star formation occurring in Knot B (Jackson et al. 2012). We can put an upper limit on the black hole mass using the (5σ) upper limit to the radio flux from Heisler et al. (1998) and the X-ray-radio black hole "fundamental plane" (Merloni et al. 2005). Assuming a 2.3 GHz GHz flux of <3.8 mJy, and further assuming that any compact core has a flat spectrum so that $S_{5\ \mathrm{GHz}} \sim S_{2.3\ \mathrm{GHz}}$, we derive a black hole mass of $< 5 \times 10^7\ M_\odot$.

Adamo et al. (2010) estimate that the star formation in Knot B has been on-going for ∼3.5 Myr. If there is a supermassive

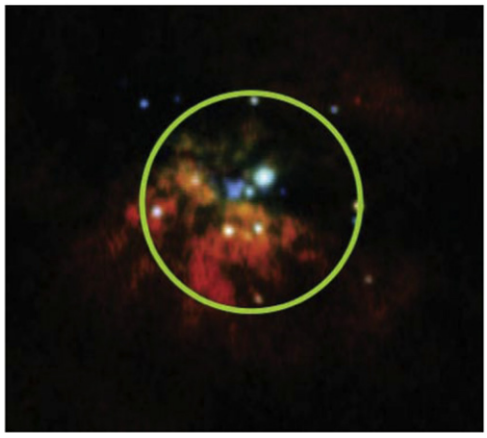

Figure 7. *Chandra* image of the starburst core of M82. The brightest source is M82 X-1. The compact source Haro 11 X-1 may comprise a very luminous source similar to M82 X-1 plus residual emission from the surrounding starburst. The green circle shows the area encompassed by a 1 arcsec aperture of the distance of Haro 11.

black hole buried in Knot B, it is unlikely to have formed in the current star formation event, which is probably triggered by a galaxy merger. The seed black hole must have been present in one of the galaxies prior to the merger, and it is now being fueled by the starburst and merger process.

3.2.2. One or More X-Ray Binaries: an IMBH?

One or more X-ray binary can naturally explain both the energetics and hard-X-ray spectrum of Haro 11 X-1. In this context, it is useful to compare the X-ray source population of Haro 11 to that of the nearby startburst galaxy M82. The central starburst region in M82 contains ∼22 sources within a 2.5 × 2.5 kpc area (Griffiths et al. 2000). The integrated flux from the point sources is dominated by M82 X-1, a single bright variable source (Kaaret et al. 2001; Matsumoto et al. 2001). In the low state, M82 X-1 contributes 30% of the flux from point sources in M82. In the high state, M82 X-1 dominates the point source flux. It seems plausible that the compact source Haro 11 X-1 is similar to the starburst region of M82, except that Haro 11 is significantly further than M82 (84 Mpc versus 3.7 Mpc) and hence individual sources are not detected and resolved. This is illustrated in Figure 7, which shows the area encompassed by a 1 arcsec aperture at the distance of Haro 11.

The very hard spectrum is consistent with Haro 11 X-1 being dominated by a single source. Gladstone et al. (2009) find that the highest quality ULX spectra can be modeled by a cool disk component together with a power law that breaks/rolls over above 3 keV. The spectrum of Haro 11 X-1 is significantly harder than any of the sources studied by Gladstone et al. (2009). It is similar to the spectra of a sample of extreme ULX ($L_X > 5 \times 10^{40}$ erg s^{-1} studied by Sutton et al. (2012). Sutton et al. (2012) suggest that extreme ULXs with relatively hard spectra may be black hole binaries in the low, hard state (see also Feng & Kaaret 2006). If we make the assumption that Haro 11 X-1 is a black hole in the low state, radiating at less than 10% of the Eddington luminosity, then the mass of the black hole is greater than $7600 M_\odot$, putting it in the "IMBH" category.

Alternately, Haro 11 X-1 could be a highly super-Eddington massive stellar BH ($M \sim 100\ M_\odot$ radiating at ∼10 times Eddington). Recently, Sutton et al. (2013) suggested that most ULXs can be explained as stellar-mass black holes accreting at and above the Eddington limit. Such high accretion rates lead to the formation of a wind or jet. The X-ray spectrum and variability characteristics depend on the accretion rate and inclination of the system. The "hard" ultra luminous state occurs when observing primarily down the jet funnel to the hard central engine. A softer component is observed from the wind at higher inclination angles. It is impossible to distinguish between these two possibilities (IMBH radiating at 10% Eddington versus super Eddington accretion onto a $100 M_\odot$ black hole) with the current data: high quality X-ray spectra (several thousand counts) are required to do the spectral fitting. This would require extremely long exposures for *Chandra* since other observatories cannot resolve Haro 11 X-1 and Haro 11 X-2.

If Haro 11 X-1 is an IMBH in a low accretion state, it has the potential to transition to a high state. If Haro 11 X-1 transitions to a high state, it will reach luminosities that will classify it as a Hyper Luminous X-ray source (HLX defined as $L_X \geqslant 10^{41}$ erg s^{-1} Gao et al. 2003). It is potentially significant that Haro 11 is a low metallicity galaxy, apparently similar to higher redshift objects. An IMBH may be a "seed" black hole that is currently growing rapidly to form a supermassive black hole (Jia et al. 2011). MacHattie et al. (2014) note that the H I line width is consistent with the rotation curve measured by Östlin et al. (1999). This suggests that the H I resides at the dynamical center of the galaxy, where one would expect to find or grow a supermassive black hole.

The ULX in I Zw 18 is another excellent candidate for an IMBH in a low-metallicity starburst (Kaaret & Feng 2013). It is also interesting to note that the HLX ESO 243-49 HLX-1 is located in the outskirts of an S0 galaxy, and may be the stripped nucleus of an accreted dwarf galaxy (Farrell et al. 2011, and references therein). Haro 11 is precisely the type of system that could be the progenitor of a "stripped dwarf nucleus." Finally, we note that there is good evidence that ULXs are more common in low-metallicity dwarf galaxies (e.g., Mapelli et al. 2010; Prestwich et al. 2013; Brorby et al. 2014). In particular, Basu-Zych et al. (2013) find that the 2–10 keV X-ray luminosity per unit star formation rate in a sample of low-redshift LBAs is elevated relative to near-solar metallicity galaxies. They attribute the excess as excess ULXs in these metal-poor systems. It is likely that Haro 11 is not unique, and that extreme ULXs/HLXs are common in LBAs.

4. THE SIGNIFICANCE OF HARO 11 X-2: XRB AND FEEDBACK IN LAE AND LBAS

The X-ray luminosity of Haro 11 X-2 is characteristic of a ULX. The X-ray spectrum (soft power law $\Gamma = 2.2$) is also consistent with the interpretation of Haro 11 X-2 as a ULX (Gladstone et al. 2009). We note that most ULXs with soft spectra have X-ray luminosities $<2 \times 10^{40}$ erg s^{-1}, making Haro 11 X-2 one of the most luminous soft ULX known. Based on the X-ray characteristics, and its association with young (age ∼10 Myr, Adamo et al. 2010) star clusters in Knot C, we conclude that Haro 11 X-2 is a stellar mass black hole ($M \sim$ 10–$100 M_\odot$, Zampieri & Roberts 2009) in a young high-mass X-ray binary.

Recent studies of ULXs with high-quality spectra have shown that a subset of these sources have soft-X-ray excesses and turnovers in the spectrum above 3 keV (Gladstone

et al. 2009). These sources can be explained in terms of super-Eddington accretion. In this scenario, a soft ultraluminous spectrum is viewed (at least in part) through a massive outflowing wind, with the softness of the spectrum due to the Compton down scattering of inner-disk photons in this very optically thick wind (Sutton et al. 2013). The wind is a direct consequence of super-Eddington accretion—the intense radiation release of the inner-disk results in a radiatively driven wind from the loosely bound surface of the accretion disk, so that it becomes geometrically thick in its inner regions (Poutanen et al. 2007; Middleton et al. 2015).

We suggest that Haro 11 X-2 is a ULX accreting in the super-Eddington state. The X-ray spectrum (soft power law $\Gamma = 2.2$) is consistent with the interpretation of Haro 11 X-2 as a super Eddington accretor (Gladstone et al. 2009). However, we note that most ULXs with soft spectra have X-ray luminosities $<2 \times 10^{40}$ erg s^{-1}. The X-ray luminosity of Haro 11 X-2 (5×10^{40} erg s^{-1}) is too high for a "standard" stellar mass black hole ($M < 20\ M_{\odot}$). It likely requires that the black hole has a mass in the range of 20–100$M_{\odot}$.

The importance of outflows/feedback in allowing Lyα to escape is widely accepted (Heckman et al. 2011; Orsi et al. 2012; Wofford et al. 2013). However, the earliest source of the outflow is assumed to be winds from supernova and high-mass stars (see the evolutionary scenario in Mas-Hesse et al. 2003) At later times, an AGN can form and also contribute. The association of Haro 11 X-2 with the Lyα emission raises the possibility that winds from the compact object may play a significant role in sweeping up the neutral gas and allowing the Lyα to escape. The mechanical luminosity in the wind of an XRB is generally comparable to the radiative luminosity (Gallo et al. 2005; Justham & Schawinski 2012): there is evidence for some systems that the mechanical luminosity might dominate the radiative luminosity by several orders of magnitude (Pakull et al. 2010).

Figure 8 shows the mechanical power from supernovae and stellar winds as a function of time for the starburst region Knot C (red curve) compared to estimated feedback from a ULX (blue curve). We use the Starburst99 code (Leitherer et al. 1999; Vázquez and Leitherer 2005; Leitherer et al. 2010) to model the mechanical power (supernova plus stellar winds) for an instantaneous starburst of fixed mass. We adopt a Kroupa (2001) initial mass function (IMF) with mass limits 0.1 and 100 $M_{\odot}$, a turnover stellar mass at 0.5 $MM_{\odot}$, and lower/upper IMF exponents of $\alpha = 1.3/2.3$. The input star cluster mass is $10^7\ M_{\odot}$ and the metallicity is $Z = 0.004$ (values are those derived for Knot C by Adamo et al. 2010). The blue line shows the mechanical power from the ULX, with the conservative assumption that the mechanical power is approximately equal to the radiative power. The wind from the ULX could turn on ~3 Myr after formation, and last for the lifetime of the binary (~10 Myr: Rappaport et al. 2010). The age of the cluster (estimated by Adamo et al. 2010) is shown in green. It is clear that a single ULX has the potential to contribute significantly to, and possibly dominate, the mechanical power.

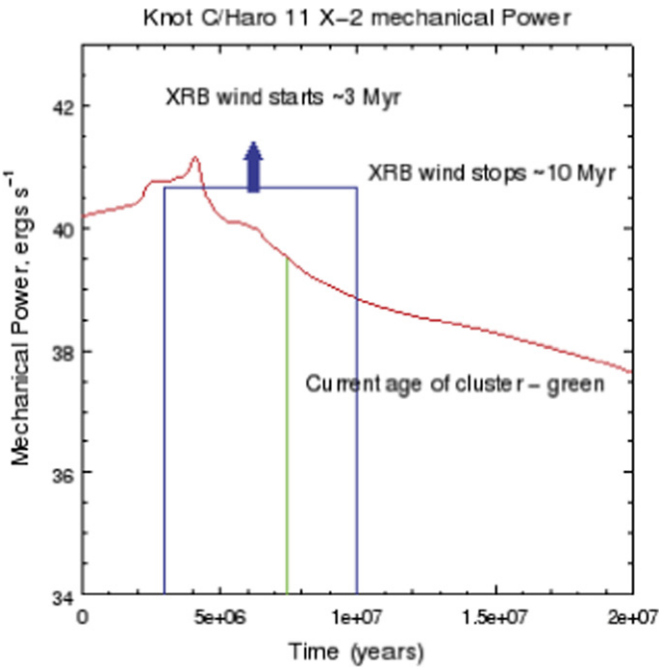

Figure 8. Mechanical power vs. time for Knot C and Haro 11 X-1. The red curve shows the mechanical power (supernovae plus stellar winds) from a 10^7 $M_{\odot}$ instantaneous burst of star formation. The age of Knot C (~10 Myr, Adamo et al. 2010) is shown in green. The blue shows the approximate mechanical power from a 5×10^{40} erg s^{-1} ULX, assuming (1) that the mechanical power ~ radiative luminosity (2) the outflow turns on when the ULX is 3 Myr old and turns off at 10 Myr. The mechanical power from a ULX may be greater than the radiative luminosity, so the blue line is a lower limit as indicated by the arrow.

5. SUMMARY AND CONCLUSIONS

We find two point sources embedded in the diffuse emission in the Lyα galaxy Haro 11.

Haro 11 X-1 is extremely luminous, spatially compact, has a hard-X-ray spectrum and is associated with Knot B and a compact H I absorption source. There is no evidence for an LLAGN in the optical or infrared emission lines, and no high surface brightness radio core. We cannot rule out an AGN whose optical and IR signatures are diluted by the intense starburst. We conclude that this source is most likely dominated by a single luminous XRB on the basis of energetics and the hard-X-ray spectrum, similar to the IMBH candidate in M82 (M82 X-1). We cannot distinguish between a stellar black hole ($M \sim 100\ M_{\odot}$) and an IMBH ($M \sim 7600\ M_{\odot}$) with current data. If Haro 11 X-1 is indeed dominated by a single BHB, the hard spectrum suggests that it is an IMBH in a low-accretion state. An IMBH may be a "seed" black hole that is currently growing rapidly to form a supermassive black hole (Jia et al. 2011).

Haro 11 X-2 is a ULX, and is most likely a young HMXB. It is associated with Knot C, and is coincident with the Lyα line emission. We suggest that winds from the ULX may play a significant role in sweeping up the neutral gas and allowing the Lyα to escape. Haro 11 is an LBA, and hence similar to LBG at high redshifts. This raises the possibility that feedback from ULXs plays an important role in allowing Lyα emission to escape from low-metallicity galaxies in the early universe.

The scientific results reported in this article are based on data obtained from the *Chandra* Data Archive. This research has made use of software provided by the *Chandra* X-ray Center (CXC) in the application packages CIAO, ChIPS, and Sherpa.

Based on observations made with the NASA/ESA *Hubble Space Telescope*, and obtained from the Hubble Legacy Archive, which is a collaboration between the Space Telescope Science Institute (STScI/NASA), the Space Telescope

European Coordinating Facility (ST-ECF/ESA), and the Canadian Astronomy Data Centre (CADC/NRC/CSA).

REFERENCES

Abolmasov, P. 2011, NewA, 16, 138
Abolmasov, P. K., Swartz, D. A., Fabrika, S., et al. 2007, ApJ, 668, 124
Adamo, A., Östlin, G., Zackrisson, E., et al. 2010, MNRAS, 407, 870
Basu-Zych, A. R., Lehmer, B. D., Hornschemeier, A. E., et al. 2013, arXiv:1306.0906
Brorby, M., Kaaret, P., & Prestwich, A. 2014, MNRAS, 441, 2346
Dickey, J. M., & Lockman, F. J. 1990, ARA&A, 28, 215
Dijkstra, M., Wyithe, J. S. B., & Haiman, Z. 2007, MNRAS, 379, 253
Farrell, S. A., Servillat, M., Wiersema, K., et al. 2011, AN, 332, 392
Feng, H., & Kaaret, P. 2006, ApJ, 653, 536
Fontanot, F., Cristiani, S., & Vanzella, E. 2012, MNRAS, 425, 1413
Fragos, T., Lehmer, B. D., Naoz, S., Zezas, A., & Basu-Zych, A. 2013, ApJL, 776, L31
Gallo, E., Fender, R., Kaiser, C., et al. 2005, Natur, 436, 819
Gao, Y., Wang, Q. D., Appleton, P. N., & Lucas, R. A. 2003, ApJL, 596, L171
Gladstone, J. C., Roberts, T. P., & Done, C. 2009, MNRAS, 397, 1836
Griffiths, R. E., Ptak, A., Feigelson, E. D., et al. 2000, Sci, 290, 1325
Grimes, J. P., Heckman, T., Strickland, D., et al. 2007, ApJ, 668, 891
Gronwall, C., Ciardullo, R., Hickey, T., et al. 2007, ApJ, 667, 79
Haiman, Z., & Spaans, M. 1999, ApJ, 518, 138
Hao, L., Wu, Y., Charmandaris, V., et al. 2009, ApJ, 704, 1159
Hargrave, P. J. 1974, MNRAS, 168, 491
Hayes, M., Östlin, G., Atek, H., et al. 2007, MNRAS, 382, 1465
Hayes, M., Östlin, G., Schaerer, D., et al. 2010, Natur, 464, 562
Heckman, T. M., Borthakur, S., Overzier, R., et al. 2011, ApJ, 730, 5
Heckman, T. M., Hoopes, C. G., Seibert, M., et al. 2005, ApJL, 619, L35
Heisler, C. A., Norris, R. P., Jauncey, D. L., Reynolds, J. E., & King, E. A. 1998, MNRAS, 300, 1111
Hoopes, C. G., Heckman, T. M., Salim, S., et al. 2007, ApJS, 173, 441
Hu, E., & McMahon, R. G. 1996, Natur, 382, 281
Jackson, F. E., Roberts, T. P., Alexander, D. M., et al. 2012, MNRAS, 422, 2
James, B. L., Tsamis, Y. G., Walsh, J. R., Barlow, M. J., & Westmoquette, M. S. 2013, MNRAS, 430, 2097
Jia, J., Ptak, A., Heckman, T. M., et al. 2011, ApJ, 731, 55
Justham, S., & Schawinski, K. 2012, MNRAS, 423, 1641
Kaaret, P., & Feng, H. 2013, ApJ, 770, 20
Kaaret, P., Prestwich, A. H., Zezas, A., et al. 2001, MNRAS, 321, L29
Kroupa, P. 2001, MNRAS, 322, 231
Kunth, D., Leitherer, C., Mas-Hesse, J. M., Östlin, G., & Petrosian, A. 2003, ApJ, 597, 263
Lacki, B. C., & Thompson, T. A. 2013, ApJ, 762, 29
Leitet, E., Bergvall, N., Piskunov, N., & Andersson, B.-G. 2011, A&A, 532, A107
Leitherer, C., Ortiz Otálvaro, P. A., Bresolin, F., et al. 2010, ApJS, 189, 309
Leitherer, C., Schaerer, D., Goldader, J. D., et al. 1999, ApJS, 123, 3
MacHattie, J. A., Irwin, J. A., Madden, S. C., Cormier, D., & Rémy-Ruyer, A. 2014, MNRAS, 438, L66
Mallery, R. P., Mobasher, B., Capak, P., et al. 2012, ApJ, 760, 128
Mapelli, M., Ripamonti, E., Zampieri, L., Colpi, M., & Bressan, A. 2010, MNRAS, 408, 234
Mas-Hesse, J. M., Kunth, D., Tenorio-Tagle, G., et al. 2003, ApJ, 598, 858
Matsumoto, H., Tsuru, T. G., Koyama, K., et al. 2001, ApJL, 547, L25
McClintock, J. E., & Remillard, R. A. 2006, in Compact Stellar X-Ray Sources, ed. W. H. G. Lewin & M. van der Klis (Cambridge: Cambridge Univ. Press), 157
Merloni, A., Heinz, S., & Di Matteo, T. 2005, Ap&SS, 300, 45
Mesinger, A., & Furlanetto, S. R. 2008, MNRAS, 386, 1990
Middleton, M. J., Heil, L., Pintore, F., Walton, D. J., & Roberts, T. P. 2015, MNRAS, 447, 3243
Neufeld, D. A. 1991, ApJL, 370, L85
Nilsson, K. K., Møller, P., Möller, O., et al. 2007, A&A, 471, 71
Orsi, A., Lacey, C. G., & Baugh, C. M. 2012, MNRAS, 425, 87
Östlin, G., Amram, P., Masegosa, J., Bergvall, N., & Boulesteix, J. 1999, A&AS, 137, 419
Östlin, G., Hayes, M., Kunth, D., et al. 2009, AJ, 138, 923
Ouchi, M., Shimasaku, K., Akiyama, M., et al. 2008, ApJS, 176, 301
Pacucci, F., Mesinger, A., Mineo, S., & Ferrara, A. 2014, MNRAS, 443, 678
Pakull, M. W., & Mirioni, L. 2002, arXiv:astro-ph/0202488
Pakull, M. W., Soria, R., & Motch, C. 2010, Natur, 466, 209
Poutanen, J., Lipunova, G., Fabrika, S., Butkevich, A. G., & Abolmasov, P. 2007, MNRAS, 377, 1187
Prestwich, A. H., Tsantaki, M., Zezas, A., et al. 2013, ApJ, 769, 92
Rappaport, S., Levine, A., Pooley, D., & Steinhorn, B. 2010, ApJ, 721, 1348
Remillard, R. A., & McClintock, J. E. 2006, ARA&A, 44, 49
Rieke, G. H., Lebofsky, M. J., Thompson, R. I., Low, F. J., & Tokunaga, A. T. 1980, ApJ, 238, 24
Scarlata, C., Colbert, J., Teplitz, H. I., et al. 2009, ApJL, 704, L98
Servillat, M., Farrell, S. A., Lin, D., et al. 2011, ApJ, 743, 6
Shapley, A. E., Steidel, C. C., Pettini, M., Adelberger, K. L., & Erb, D. K. 2006, ApJ, 651, 688
Steidel, C. C., Adelberger, K. L., Giavalisco, M., Dickinson, M., & Pettini, M. 1999, ApJ, 519, 1
Steidel, C. C., Giavalisco, M., Pettini, M., Dickinson, M., & Adelberger, K. L. 1996, ApJL, 462, L17
Steidel, C. C., Pettini, M., & Hamilton, D. 1995, AJ, 110, 2519
Sutton, A. D., Roberts, T. P., & Middleton, M. J. 2013, MNRAS, 435, 1758
Sutton, A. D., Roberts, T. P., Walton, D. J., Gladstone, J. C., & Scott, A. E. 2012, MNRAS, 423, 1154
Tenorio-Tagle, G., Silich, S. A., Kunth, D., Terlevich, E., & Terlevich, R. 1999, MNRAS, 309, 332
Vader, J. P., Frogel, J. A., Terndrup, D. M., & Heisler, C. A. 1993, AJ, 106, 1743
Vázquez, G. A., & Leitherer, C. 2005, ApJ, 621, 695
Verhamme, A., Dubois, Y., Blaizot, J., et al. 2012, A&A, 546, A111
Wofford, A., Leitherer, C., & Salzer, J. 2013, ApJ, 765, 118
Yukita, M., Swartz, D. A., Tennant, A. F., Soria, R., & Irwin, J. A. 2012, ApJ, 758, 105
Zampieri, L., & Roberts, T. P. 2009, MNRAS, 400, 677